Evaluation of the SoilVUE10 Time Domain Reflectometry for soil water measurements in testbed field conditions

Timothy Wilson[1], John Kochendorfer[2], Howard Diamond[2], Tilden Meyers[2], Mark Hall[1], Brent French[1], Latoya Myles[2], and Rick Saylor[2]
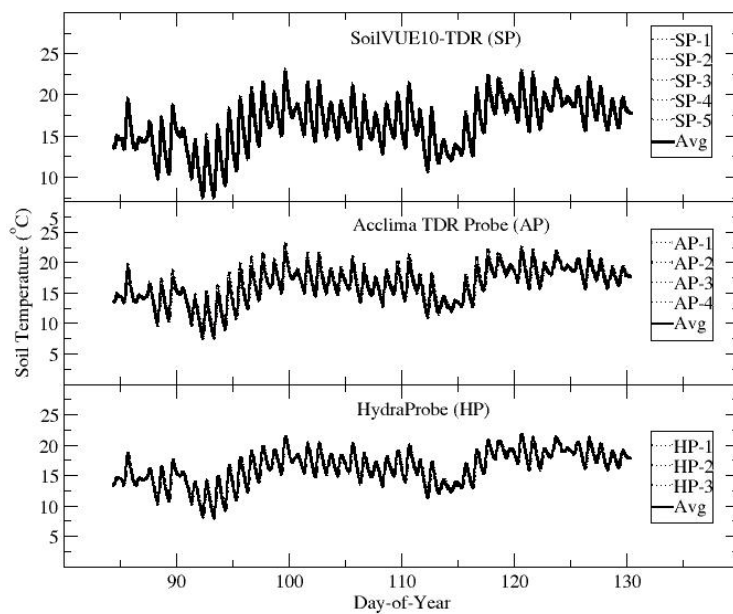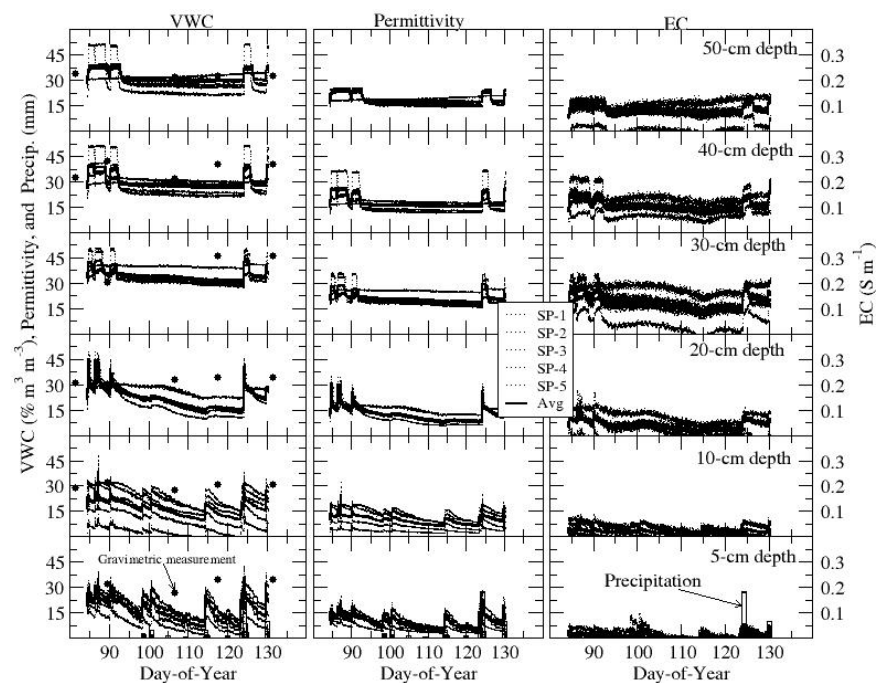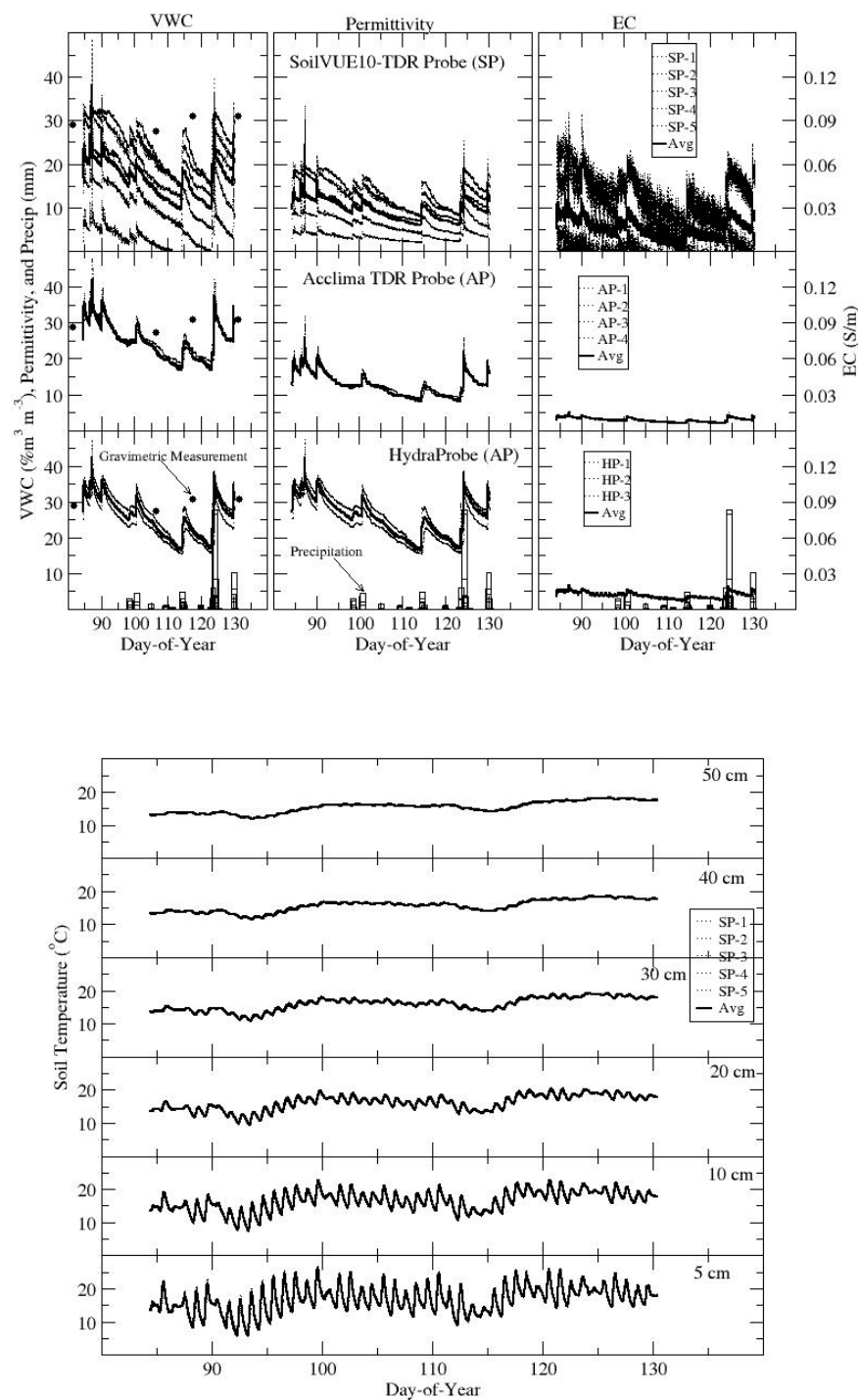
[1]NOAA
[2]NOAA-ARL

November 25, 2022

Abstract

The U.S. Climate Reference Network (USCRN) has been engaged in ground-based soil water and soil temperature measurements since 2009. As a nationwide climate network, the network stations are distributed across vast complex terrains. Due to the expansive distribution of the network and the related variability in soil properties, obtaining site-specific calibrations for sensors is a significant and costly endeavor. Presented here are three commercial-grade electromagnetic sensors, with built-in thermistors to measure both soil water and soil temperature, including the SoilVUE10 Time Domain Reflectometry (TDR) probe (hereafter called SP, for SoilVUE Probe) (Campbell Scientific, Inc., Logan, UT), the 50 MHz coaxial impedance dielectric sensor (model HydraProbe (hereafter called HP), Stevens Water Monitoring Systems, Inc., Portland, OR), and the TDR-315L Acclima Probe (hereafter called AP) sensor (model TDR-315L, Acclima, Inc., Meridian, ID), which were evaluated in a nonconductive loam soil in Oak Ridge, Tennessee, USA from 2021 to 2022. The manufacturer-supplied calibration equation for loam soils was successfully used in this study. Measurements of volumetric water content by SP were much lower than gravimetric measurements in the top 20-cm soil horizon, where soil water showed relatively large spatial variability. Study results highlight that the SP may be an important alternative to reduce soil disturbances that usually ensue when HP and AP sensors are installed; however, in-situ calibrations are essential for the SP for xeric soil water conditions.

Hosted file

`essoar.10512035.1.docx` available at https://authorea.com/users/553684/articles/605307-evaluation-of-the-soilvue10-time-domain-reflectometry-for-soil-water-measurements-in-testbed-field-conditions

1

Evaluation of the SoilVUE10 Time Domain Reflectometry for soil water measurements in testbed field conditions

Timothy B. Wilson[a1], John Kochendorfer[a], Howard J. Diamond[b], Tilden P. Meyers[a], Mark Hall[a], Brent French[a], LaToya Myles[a], and Rick D. Saylor[a]

[a] *NOAA/Air Resources Laboratory/ORAU, P.O. Box 2456, Oak Ridge, TN 37831*

[b]*NOAA/Air Resources Laboratory, 5830 University Research Court, College Park, MD 20740*

Core ideas

- This study evaluated volumetric soil water content measurements at depths of 5, 10, 20, 30, 40, and 50 cm inside a custom-built soil testbed in Oak Ridge, Tennessee, USA.

- The SoilVUE10 TDR was compared with the 50 MHz HydraProbe and the Acclima 1 GHz Time-Domain Reflectometry (TDR)-315L.

- The comparison of automated sensor volumetric soil water content with gravimetric measurements revealed that the SoilVUE10 TDR was less accurate than the Acclima TDR-315Ls and the HydraProbe within the top 20-cm soil horizon where the soil water dynamics showed large variability.

Abstract

The U.S. Climate Reference Network (USCRN) has been engaged in ground-based soil water and soil temperature measurements since 2009. As a nation-wide climate network, the network stations are distributed across vast complex terrains. Due to the expansive distribution of the network and the related variability in soil properties, obtaining site-specific calibrations for sensors is a significant and costly endeavor. Presented here are three commercial-grade electromagnetic sensors, with built-in thermistors to measure both soil water and soil temperature, including the SoilVUE10 Time Domain Reflectometry (TDR) probe (hereafter called SP, for SoilVUE Probe) (Campbell Scientific, Inc., Logan, UT), the 50 MHz coaxial impedance dielectric sensor (model HydraProbe (hereafter called HP), Stevens Water Monitoring Systems, Inc., Portland, OR), and the TDR-315L Acclima Probe (hereafter called AP) sensor (model TDR-315L, Acclima, Inc., Meridian, ID), which were evaluated in a nonconductive loam soil in Oak Ridge, Tennessee, USA from 2021 to 2022. The manufacturer-supplied calibration equation for loam soils was successfully used in this study. Measurements of volumetric water content by SP were much lower than gravimetric measurements in the top 20-cm soil horizon, where soil water showed relatively large spatial variability. Study results highlight that the SP may be an important alternative to reduce soil disturbances that usually ensue when

HP and AP sensors are installed; however, in-situ calibrations are essential for the SP for xeric soil water conditions.

1 Corresponding author

E-mail address: tim.wilson@noaa.gov

1. Introduction

Passage of the 2006 National Integrated Drought Information System (NIDIS) Act that was reauthorized in 2018 by the United States Congress mandated the National Oceanic and Atmospheric Administration (NOAA) to improve the United States drought early warning system (NIDIS Reauthorization Act of 2018, Public Law 115-423, 132 STAT 5454 (NIDIS, 2019)). Soil water is a key variable for monitoring drought (Hubbard and Wu, 2005; Moeletsi and Walker, 2012) and providing high quality soil water data is essential to other applications such as weather forecasting, climate predictions, hydrology modeling, flood predictions, ecology studies, wildfire predictions, and agriculture operations (Torres et al., 2013; Sciuto and Diekkruger, 2010; Brye et al., 2000; Morgan et al., 2003; James et al., 2003; Cheng and Cotton, 2004; Crow and Wood, 2002; Robinson et al., 2008; Mittelbach et al., 2011; Jones et al., 2017). The United States Climate Reference Network (USCRN) was first operationally commissioned in 2004 (based on the experience in operating 40 pre-commissioned stations since 2000) in order to provide long-term, standardized measurements of air temperature and precipitation (Diamond et al., 2013). In support of NIDIS' mission, USCRN dramatically expanded its operation in 2009 by adding measurements of soil temperature and soil water content using permanently installed 50 MHz Coaxial Impedance Dielectric HP sensors (Bell et al., 2013). At the time HP sensors were among the best commercially available electromagnetic sensors for measuring soil water (Seyfried and Murdock, 2004; Jones et al., 2005; Seyfried et al., 2005; Seyfried and Grant, 2007) as per evaluation at a formal soil sensor workshop conducted in Oak Ridge, TN, in 2009, where this determination was made based on a combination of cost, performance, and usage in other observing networks.

Advances in electromagnetic sensor technology continue to grow, and the ability to incorporate new sensors into soil networks to improve soil water measurements is a challenge. The deployment of new sensors often requires calibration and validation in order to be adopted or incorporated in existing networks such as the USCRN without introducing discontinuity or heterogeneity in the measurement record. Adoption of improved soil sensor technology may also be advanced by evaluating soil water sensors in testbed settings for use by soil networks in order to relieve network operations of the burden of on-site calibration and validation of sensors. This opportunity has motivated many testbed studies that have evaluated how electromagnetic sensor performances are affected by various factors, including temperature, water content, soil types, soil electrical

conductivity, sensor operation frequencies, and sensor design (Or and Wraith, 1999; Robinson et al., 2003; Seyfried et al., 2005; Dirksen and Dasberg, 1993; Logsdon et al., 2010; Burns et al., 2014; Dettman and Bechtold, 2018; Schwartz et al., 2013; 2016; Sheng et al., 2017). Examples of studies that have focused on the problem of producing on-site calibrations for soil networks include the Soil Moisture Active Passive Mission, Marena, Oklahoma, In Situ Sensor Testbed (SMAP-MOISST) (Cosh et al., 2016), the NOAA Hydrometeorology Testbed (HMT) program in AZ and CA (Zamora et al., 2011), soil-specific calibrations of sensors for the National Ecological Observatory Network (NEON) in laboratory settings using site-specific soil samples (Roberti et al., 2018); and the evaluation of TDR AP against HP for the USCRN operation using a testbed in Oak Ridge, TN (Wilson et al., 2020).

The USCRN soil water measurements currently do not include site- and soil-specific calibrations of the soil sensors for individual soil depths. Direct measurements of in situ soil properties are scarce, and we are aware of no calibration of soil water permittivity methods that explicitly include soil electrical conduction. Instead, the USCRN operation continues to rely on the manufacturer-recommended calibration for loam soils to convert sensor measurements of soil dielectric permittivity to soil volumetric water content. This is mainly because it is labor-intensive to conduct on-site calibrations across the USCRN, which currently includes 114 stations in the continental United States, 23 stations in Alaska (29-30 stations by 2026), and two stations in Hawaii (Diamond et al., 2013). In the eastern and central United States, many USCRN stations are located on agricultural research and conservation land sites; in the western United States, most stations are sited on federal land reserves consisting of national parks, forests, grasslands, and wildlife preserves. Network site conditions are therefore highly diverse in terms of soil, vegetation, climate, soil texture, bulk density, soil structure heterogeneity, soil moisture, and soil temperature. The large and diverse distribution of the network sites has hampered accurate quantification of the role of the local soil conditions on soil dielectric permittivity measurements across the individual USCRN sites and soil depths. For instance, unlike the soil dielectric permittivity variables that are measured continuously and automatically, gravimetric measurement (which is the standard approach to validate other soil water content methods) is not amenable to remote or automatic observations. It requires manually collecting soil samples and analyzing them using intensive laboratory protocols. Performing repeated manual soil sampling is impractical for the USCRN due to the additional labor, cost, and travel considerations. In addition, extracting numerous soil samples from the soil profile alters the soil matrix. Repeated sampling normally cannot be made without disturbing the soil, which could cause detrimental changes in soil structure, temperature, and soil water dynamics.

A second concern is that the assessment of the USCRN soil water measurements over the last decade has revealed the importance of not only the accuracy of the soil sensors but also their robustness and durability. Sensor failures are a critical concern to the USCRN and similar observational networks. Sensor

failures can result in data gaps and spurious results in soil measurement time series. In addition, sensor replacement and reinstallation consume network resources. The USCRN is unique in that redundant soil probes are deployed at each measurement depth, but even this approach has not proven to prevent data discontinuities when events like lightning strikes damage multiple sensors at once. The causes of soil sensor failures or erroneous measurements are diverse, complicated, and vary among sites (Jones et al., 2005). Vaz et al. (2013) reported that the sensitivity of dielectric permittivity sensors to soil type depends on the sensor type, specific electronics, circuitry, and probe size and design. Sensor performance issues also include effects from sensor hardware and software internal calibrations and corrections (Sakaki & Rajaram, 2006).

Reported evaluations of the USCRN soil measurements have included the technical description of the network soil observations (Bell et al., 2013), a detailed overview of USCRN as the preeminent national climate monitoring network (Howard et al., 2013), the analysis of soil properties of individual network sites and individual soil measurement depths (Wilson et al. 2016), and the evaluation of the benefit of replacing HP with TDR AP in the network (Wilson et al., 2020). The network continues to provide high quality soil water data, but challenges remain, especially for sites with soils that display effects of high electrical conductivity (EC). In particular, many USCRN sites with high clay content soils that experience wet conditions on a consistent basis have imposed difficulties on electromagnetic sensor measurements (Wilson et al., 2020).

Many other studies have reported that fine clay soils with high electrical conduction exhibit consistent dielectric dispersion regardless of the sensor measurement frequency (Logsdon & Laird, 2004; Saarenketo, 1998). Many of these studies have evaluated how the temperature can also influence the soil electrical conduction and ultimately water permittivity measurements (Jones et al., 2005; Blonquist et al., 2005; Seyfried and Murdock, 2004; Seyfried and Grant, 2007). While most dry soil minerals are nonconductors, when these soil particle grains absorb water molecules, the interaction forms electrolytes in the soil-water mixture around the soil particles, and the applied electromagnetic field induces electrical conduction. As ion concentration increases in the soil water content (e.g., soils with high cation exchange capacity and specific surface area), EC tends to increase in proportion to the applied electromagnetic field, and this increase may hinder the soil water permittivity measurement; both the imaginary and real components of permittivity can increase, especially when measured at frequencies less than 100 MHz (Robinson et al., 2003; Vaz et al., 2013; Seyfried et al., 2005; Seyfried and Murdock, 2004; Kelleners et al., 2009; Ojo et al. 2015). In addition, the physical properties of fine clay soils, such as surface area, particle shape, and soil structure layering, can produce errors in dielectric permittivity measurements, and ultimately in soil water content determination (Jones et al., 2005; Schwartz, Evett, & Bell, 2009; Schwartz, Evett, Pelletier, & Bell, 2009).

Since 2009, the Time Domain Reflectometry (TDR) AP sensors which operate at a much higher frequency (about 1 GHz) than the HP have gained broad ac-

4

ceptance over low frequency sensors like the HP, and AP sensors were integrated into USCRN in 2019 (Wilson et al., 2020). The TDR sensors that operate at frequencies >1 GHz have demonstrated less sensitivity to soil electrical conduction compared to electromagnetic sensors that operate at far lower frequencies like the HP, which operates at 50 MHz (Seyfried and Murdock, 2004); TDR sensors are therefore well regarded among the available soil moisture measurement sensors. In addition, advances in the development of dielectric permittivity sensors have continued to produce new models of TDR sensors since TDR AP sensors were added to USCRN soil measurements. Some newer TDR sensors are becoming less expensive than the TDR AP and may provide the same level of accuracy as the TDR AP with the potential for improved soil moisture network operations.

In this study, a soil testbed in Oak Ridge, TN, was employed to evaluate the benefits of using select commercially available electromagnetic sensors for measuring soil water in the USCRN. The specific objectives are as follows: (1) evaluate the recently developed Campbell Scientific SP against both the AP and the HP sensors in the testbed; and (2) explore the benefits of using the SP as an alternate sensor for the USCRN soil measurements. The SP sensors are similar to AP sensors, and both are thermistor and true TDR soil moisture sensors with SDI-12 communications. However, the SP design consists of the TDR circuitry of individual helical waveguides embedded in a threaded cylinder that incorporates multiple nodes to measure the vertical profile of soil water content, soil temperature, dielectric permittivity, and electrical conductivity. The SP are available in lengths of 50 cm with 6 measurement points, and 100 cm with 9 measurement points. The SP therefore allows for one probe to monitor the soil vertical profile which would otherwise require several individual AP or HP. For the USCRN, which must sustain sensors in nationally distributed stations, the SP may be an excellent alternate sensor with the potential to reduce not only network operation cost but also the labor and soil disturbance associated with sensor installation.

2. Methods

2.1. Field measurements

To evaluate the SP performance, field measurements were made during 2021 to 2022 in a research soil testbed near Oak Ridge, Tennessee USA (36° 0´ N, 84° 14´ 25 W) that was established in 2016. The testbed has settled well in the landscape. The site is an open urban grassy field, homogeneous over several meters, with tree lines about 10 m to the east and over 100 m to the south. The site elevation is about 303 m above MSL. The soil at the site is classified under the USDA system as a Montevallo channery silt loam, 20-35% slope. The average of soil factors in the top 1 m shows a cation exchange capacity (CEC) of about 3.8 cmol/kg, a bulk density of 1.35 mg m^{-3}, and a pH of about 4.9. The testbed was exposed to the ambient conditions of the area. The climate is temperate with long hot-humid summers and short mild winters. The normal monthly temperature varies from about 5 ° C during the winter and early spring

to peak values of about 23 °C during the summer, and then gradually decreases again to about 15 °C during the fall. The region normally receives about 1300 mm of annual precipitation; the maximum normal monthly precipitation of 130 mm occurs during the winter and early spring, and normal monthly precipitation values of 116 and 100 mm occur during summer and fall, respectively. The predominant wind direction at the area is out of the south-southwest, and the primary source of moisture for the area is the Gulf of Mexico.

Wilson et al. (2020) provided a detailed description of the testbed in which the AP was evaluated against the HP. The testbed, which covered a rectangular area measuring 1.3 m x 2.45 m and was about 0.2-m above the natural ground of a relatively flat grassy lawn, was a uniformly packed loamy soil to reduce the errors associated with soils that have high electrical conductivity. A dense grass cover was maintained across the testbed to provide uniform surface cover over the testbed and to enhance uniform wetting and drying in the testbed. Beginning in March 2021, five 50-cm SP sensors with measurement depths centered at 5, 10, 20, 30, 40, and 50 cm, respectively, were buried vertically alongside four HP sensors and four AP sensors that were installed horizontally in the testbed at a depth of 0.1-m since 2016. The sensors were spaced about 0.25 m horizontally apart. The probes were installed with minimum disturbance to the testbed. To install the SP, a 5 cm diameter hand operated auger was used to drill a hole, and the threaded sensor probe was screwed into the hole. Variables measured by the HP sensors included the imaginary dielectric permittivity, the real dielectric permittivity, soil temperature (C), bulk electrical conductivity (S/m) without temperature correction, and bulk electrical conductivity (S/m) with temperature correction. With the TDR sensors (AP and SP), variables that were recorded included the volumetric water content (VWC, %m^3 m^{-3}), soil temperature (C), relative dielectric permittivity, soil bulk electrical conductivity (uS/m) and soil pore water electrical conductivity (uS/m). The real/relative dielectric permittivity values were converted to VWC values based on the sensor calibration equation by Seyfried et al. (2005), where VWC = $(0.109(\text{dielectric})^{0.5} - 0.179$, dielectric $>=2.7$ and 0, for dielectric < 2.7. A data recorder was used to supply 12 volts DC to the SDI-12 port of the sensor. Measurements at each soil depth were sampled every 5 s, averaged over 15 min, and stored by the datalogger.

To obtain independent soil water content data for the evaluation of the sensor measurements, gravimetric soil water content was measured using soil cores collected occasionally from the testbed during 2021. An AMS slide hammer soil core sampler (AMS, Inc., American Falls, Idaho) was used to collect three soil cores of a cylindrical volume of 90.43 x 10^{-6} m^3 with diameter 0.048 m and length 0.05 m. Soil cores were collected at the sensor measurements depths. Each core sample was stored inside a 0.05-m x 0.048-m-diameter cylindrical metal sleeve. Metal sleeves with soil samples were tightly sealed to prevent moisture loss. Care was taken to avoid sampling impact to the testbed by carefully backfilling all the sampling holes with the same loamy soil. Metal sleeves with soil samples were immediately weighed, and the samples were dried at 105°C to determine the soil

dry weight. The weight of the fresh soil sample, soil dry weight, and the volume of the soil core were used to calculate the gravimetric soil water content and the bulk density. In order to minimize the disturbance of the testbed soil condition, it was not possible for us to conduct regular gravimetric measurements. Instead, we evaluated gravimetric soil water content by collecting soil samples from the testbed on an occasional basis from 2021 to 2022.

2.2. The analysis of sensor measurements

The SP, AP and HP testbed measurements of dielectric permittivity, soil water content, soil temperature, and electrical conductivity were compared. Data were available during March 2021 to March 2022 for the individual soil depths, which were averaged over 15 minutes. The occasional gravimetric soil water content measurements were compared with corresponding sensor measurements. To assess the consistency of the testbed measurements in terms of each sensor type, corresponding 15-minute measurements were compared for each sensor type. To evaluate the performance of the SP sensors relative to the AP and HP, comparisons were made for the 5-minute measurements at 10 cm averaged for each group of sensors. The sensor measurement values were analyzed by calculating the root mean square difference (RMSD), the correlation coefficient (R), and the mean absolute percentage difference (MAPD) for each depth, using the gravimetric measurements as a reference. The RMSD and MAPD represent the absolute accuracy of one sensor compared with another at a given depth, while the R quantifies the variability between a pair of sensors.

2.3. The HydraProbe (HP)

The HP consists of four 57 mm long stainless-steel rods of 3 mm diameter extending from a 40 mm diameter cylindrical head. The four rods are configured with a centrally located rod surrounded by three other parallel rods forming an equilateral triangle with 22 m sides. The electronic components include a wave signal generator, thermistor, microprocessor, and communications embedded in circuitry within the cylindrical head. The thermistor is located in the stainless-steel base plated between the rods, and is used to measure the soil temperature. The stainless-steel base is in close contact with the soil when the probe rods are inserted in the soil. The accuracy of the HP is ±0.3 °C for temperature from -30 to 60 °C. In the operation of the HydraProbe, voltage signals at 50 MHz are generated by a wave generator in the probe head, transmitted to the rods via a waveguide and applied to the soil volume. The applied electromagnetic signal induces a standing wave with amplitude that decreases as soil permittivity increases. Electronics in the sensor head measure the amplitudes of the emitted signal and of the standing wave and calculate the ratio of these. The HP uses "algorithms to convert the signal response of the standing radio wave into the dielectric permittivity" (Stevens Water Monitoring Systems, 2018). The HP output measurements of the real dielectric permittivity, imaginary dielectric permittivity, electrical conductivity, and the soil temperature. The accuracy of the HP is in the range of ±0.01 to 0.03 m^3 m^{-3} for the measurement of volumetric soil water content (Stevens Water Monitoring Systems, Inc., 2018).

2.4. The TDR-315 and TDR-315L Probes (AP)

The Acclima TDR-315 and TDR-315L sensors are considered true TDR sensors. TDR-based probes determine the dielectric permittivity of the soil water by measuring the travel time of electromagnetic wave signals applied to the soil. The TDR-315 sensor consists of three 0.15 m long stainless-steel rods about 3.5 mm diameter with about 0.02 m rod spacing, attached to a 0.059 x 0.053 x 0.015 m head. Like the HP, the TDR-315 electronics are embedded in a miniaturized circuit board within the probe head, and sensed data are transmitted using the SDI-12 communication protocol via a waterproof cable. A precision thermistor is located within the central stainless-steel rod for a soil temperature measurement with a ±0.3 °C accuracy over the range of -12 to 50 °C. Both the TDR-315 and HP sensors report dielectric permittivity, bulk electrical conductivity, and soil temperature; unlike the HP, the TDR-315 measures the relative dielectric permittivity. Past publications describe the formulation and operation of TDR devices in greater detail (Robinson et al., 2003; Kelleners et al., 2009). The TDR-315 was evaluated by Schwartz et al. (2016), who described its mode of operation and advantages over conventional TDR systems.

2.3. The SoilVUE 10 TDR Probe (SP)

The SP is also based on a true TDR concept just as the TDR-315 (Robinson et al., 2003; Kelleners et al., 2009). Unlike the TDR-315, however, the SP TDR consists of a long-threaded probe designed to be installed vertically into an augured hole in the soil to measure a continuous vertical profile of the relative dielectric permittivity, volumetric water content, electrical conductivity and soil temperature at specified depths along the length of a single probe. Currently, the SP sensor is available in two length classes: one class is a 50-cm probe with 6 measurement depths at 5, 10, 20, 30, 40 and 50 cm, and the other class is a 100-cm probe with 9 measurement depths at 5, 10, 20, 30, 40, 50, 60, 75 and 100 cm; the 50-cm probe was used in this study. Thus, a single 50-cm (or 100-cm) SP can replace six (nine) individual AP or HP sensors. The diameter of the probe is 5.2 cm without the threads and is 5.8 cm including the threads. Measurements are made using a set of three individual waveguides (stainless-steel rods) embedded in the threads spaced 1.5 cm apart and centered about each specified depth. In this study, to thread the SP into the soil, we first used a handheld auger as suggested by the manufacturer to dig a hole about 5 cm in diameter and about 5 cm deeper than the length of the 50-cm long SP. A SoilVUE 10 SDI-12 cable was used to connect the probe to a Campbell Scientific, Inc. data logger. SDI-12 instruction protocols prompted the probe to make measurements at each soil depth and to retrieve the measured values, which were stored by the logger.

3. Results

Time series of the 15-minute averages of the soil volumetric water, electrical conductivity and soil temperature at a depth of 10 cm within the testbed are presented here, with the corresponding gravimetric soil water measurements.

Time series and vertical profiles of soil volumetric water, temperature, and electrical conductivity measurements by the SoilVUE 10 at 5, 10, 20, 30, 40 and 50 cm are then shown. Finally, we present the RMSE, MAPD, and 1:1 regression relationship among the HP, AP and SP.

3.1. Time series of VWC (and BSP) at depth of 10 cm

A time series of the 15-minute volumetric water content (VWC) in the top 10 cm is presented in Fig. 1 with the bulk soil permittivity (BSP), observed gravimetric soil water, and precipitation at the testbed site for 46 days from DOY 85 to 130, 2021. Measured and observed VWC are listed in Table 1. Gravimetric soil water was collected only occasionally and values were greater than the sensor measurements. Measurements of VWC by SP were lower than measurements by HP, AP, and the gravimetric soil water content (Fig. 1). Values of VWC showed clear hourly variability that increased during precipitation followed by dry-down largely consistent with high drainage and evapotranspiration. Measurements of VWC by HP, AP and SP were consistently lower than the observed gravimetric soil water content. Considering that the sensors determined VWC using manufacturer-supplied calibration equations, the performance by the all three sensors compared with the gravimetric water showed RMSD of about 9 $\%\text{m}^3\ \text{m}^{-3}$ for SP and around 2 $\%\text{m}^3\ \text{m}^{-3}$ for HP and AP. The high infiltration and drainage within the testbed resulted in relatively short periods of saturation during high precipitation events. The spatial variability of VWC was small for HP and AP, as both showed similar VWC with magnitudes clustered about the 15-minute mean value. However, VWC measurements by SP were more variable spatially, as indicated by the replicate SP measurements. The spatial heterogeneity caused by effects of the testbed grass cover on drainage and evapotranspiration dynamics showed less impact on VWC measurements by HP and AP than on VWC measurements by SP, which showed relatively large spatial variability.

3.2. Time series of VWC (and BSP) at depth of 5, 10, 20, 30, 40 and 50 cm

Fig. 2 shows the 15-minute VWC (with the permittivity) by the five replicates of SP at depths of 5, 10, 20, 30, 40 and 50 cm from DOY 85 to 130, 2021. Values of VWC showed the largest variability at 5, 10 and 20-cm depths that ranged from about 0 to 45 $\%\text{m}^3\ \text{m}^{-3}$ about a mean value of 15 $\%\text{m}^3\ \text{m}^{-3}$. This variability resulted from evapotranspiration and the coarse loam soil texture that allowed for high drainage rates. The VWC at the 30, 40 and 50 cm depths showed less variability, as VWC remained high and values did not drop below 30 $\%\text{m}^3\ \text{m}^{-3}$.

3.3. Time series of electrical conductivity (EC)

Measurements of the related EC in the testbed showed consistently low values (Figs. 1 and 2). Despite the low EC, with values less than 0.2 S m^{-1}, EC varied with VWC and tended to increase with soil depth. During the study period, EC typically increased with VWC during precipitation events. This increase of EC with VWC has important implications for electromagnetic sensors because they

assume constant low EC values, which is false for certain types of clay soils, e.g., smectite clay soils (Robinson et al., 2003; Vaz et al., 2013).

3.4. Soil temperature measurements

The time series of the soil temperature measurements by HP, AP and SP in the testbed are presented in Figs. 3 and 4. Close examination showed that soil temperature measurements were essentially equal in magnitude for all three sensors at the various depths. Fig. 5 shows the 1:1 regression relationship with no significant statistical difference between all three sensors. Our finding demonstrates the ability of all three sensors to measure the 15-minute soil temperature in the testbed. Unlike VWC, soil temperature measurements by SP did not show much variability between replicate measurements. In general, the difference in soil temperature measurements among the replicate SP sensors at each depth was minor, and the sensors all measured the soil temperature profile within the testbed well (Table 2).

3.5. Profiles of VWC, temperature, and EC

Fig. 6 shows the profile of VWC, temperature, and EC measurements by SP at 5, 10, 20, 30, 40 and 50 cm during the entire study period from 2021 to 2022. The variability of VWC was larger at 5, 10, and 20 cm (with VWC ranging from 5 to 45 $\%m^3$ m^{-3}) than at 30, 40 and 50 cm, where the VWC remained above 30 $\%m^3$ m^{-3}. The soil temperature showed only a slight decrease with depth from 5 to 50 cm.

3.6. Comparisons of VWC measurements by HP, AP and SP

We evaluated the 15-minute difference between the mean and the replicate measurements of VWC and temperature by HP, AP and SP, respectively, at 5, 10, 20, 30, 40, and 50 cm for the study period from 2021 to 2022. Table 3 provides the RMSD and MAPD for VWC and temperature. The VWC measurements by SP showed the largest difference in VWC among replicate sensors, reaching RMSD = 10.91 $\%m^3$ m^{-3} and MAPD = 65.17% at the top 10 cm, compared with RMSD < 6 $\%m^3$ m^{-3} and MAPD < 20% at 30, 40, and 50 cm. For the temperature, the differences among replicate sensors were minor for all three sensor types, where the RMSD and MAPD were less than 0.5 °C and 5%, respectively, and all three sensors performed well in the measurement of soil temperature in the testbed.

We compare the HP, AP and SP measurements of VWC with observed gravimetric soil water content at 10 cm (Fig.7), and the raw dielectric permittivity measurements by both HP and AP with measurements by SP (Fig.8). The variation of VWC measurements by the sensors was consistent with that of the gravimetric observations. Measurements of VWC by both HP and AP were in good agreement with the observed gravimetric soil water, and with each other. The 1:1 regression relationship between measured and observed VWC showed slope = 0.92, R^2 = 0.87, RMSD = 2.0, and intercept = 0.92 for the HP; slope = 0.87, R^2 = 0.80, RMSD = 2.39, and intercept = 2.00 for the AP; slope =

0.91, $R^2 = 0.82$, RMSD = 9.74, and intercept = -6.96 for SP, where SP VWC measurements were consistently lower than gravimetric values. This discrepancy may have resulted from effects of SP designs in hardware and software internal calibrations and corrections. It may have also resulted from the relative difference in the interaction between the different sensor probes and the soil characteristics in the top 10 cm in the testbed. For instance, even though both SP and AP are TDR sensors, they represent two different configurations of the soil sensing rods. The AP is made of three 15-cm long sensing rods, while the SP consists of three 2.5-cm diameter sensing rods coiled about marked points along the length of the 50 cm long SP probe. Such different configurations may have led to different sampling volumes of soil by both configurations, which may have ultimately resulted in different dielectric permittivity measurements between SP and AP.

3. Discussion

In this study, we evaluated HP, AP and SP measurements of VWC, temperature, and EC in a uniform coarse-loam soil testbed with dense grass cover in an urban grassy field in Oak Ridge, Tennessee, during March 2021 to March 2022. Measurements by both HP and AP in the top 10 cm were nearly equal during the entire study where VWC averaged about 35 %m^3 m^{-3} at the field capacity level and about 45 %m^3 m^{-3} at soil saturation. The 15-minute time series showed patterns of VWC with rapid increase during precipitation and a gradual decrease during dry-down periods. Values of VWC during the entire study period ranged from about 5 %m^3 m^{-3} for dry soil conditions to about 45 %m^3 m^{-3} for saturation conditions with heavy precipitation. The lowest VWC existed in the top 20 cm, but values did not decrease below 30 %m^3 m^{-3} at depths of 30 to 50 cm. The finding for HP and AP was very similar to measurements previously reported by Wilson et al. (2020). However, the VWC measurements by SP were lower than values by both HP and AP, even though all three were nearly equal in the measurements of temperature and EC. This discrepancy may have resulted from the differences in the design of the sensing rods between SP (three sensing rods spiraled around a 50 cm long, 2.5-cm diameter probe at each specified distance along the probe) and both HP (5.8-cm long sensing rods extended from 4-cm diameter cylindrical head) and AP (three 15-cm long sensing rods extended from 3.8-cm wide head), as well as the software internal calibrations and corrections. The larger? sampling volumes of the soil by the HP and AP may have made it possible for them to successfully measure VWC at 10 cm. The low measurements of VWC in the top 10 cm by SP may have resulted from the large variability in the soil water content that likely reduced the sampling volume of the soil by SP sensing rods, which may have limited the ability of SP to accurately aggregate the soil water variability to successfully measure VWC. The large variability of soil water at 10 cm mainly resulted from drainage and evapotranspiration dynamics that characterized the top 20 cm of the testbed.

Among the three probe types that were tested, soil temperature measurements were in better agreement than the soil volumetric water content within the

testbed. All three sensors use a precision thermistor to measure the soil temperature. Differences among replicate sensors were minor for all three sensors, with RMSD and PMD less than 0.5 C and 5%, respectively, and all the sensors performed well in the measurement of soil temperature in the testbed. Unfortunately, independent measurements of temperature were not available to compare against the sensor measurements. But our findings demonstrate the ability of all three sensors to measure the soil temperature in the testbed. In general, the soil temperature measurements did not show much spatial variability, and the soil temperature profile showed only a slight decrease with depth from 5 to 50 cm. Soil temperature data within the testbed for this study were consistent with the previous study within the testbed by Wilson et al. (2020).

One of the unique components of this study was that the relatively low values of measured EC in the testbed support the ideal notion that measurements of VWC in the testbed were not affected by EC. Despite the low EC values in our study, with EC values less 0.2 S/m, EC is well known to vary depending not only with soil type but also with soil mineralogy (e.g., Smectite clays), temperature, and soil water content; several laboratory, field and modeling studies have been widely used to evaluate the susceptibility of electromagnetic sensors to EC (Schwartz et al., 2013; 2016; Saarenketo, 1998; Or and Wraith, 1999; Logsdon and Laird, 2004; Seyfried and Grant, 2007; Seyfried et al., 2005; Robinson et al., 2003).

While advances in AP and SP have improved the methods used to determine VWC in many complex soil-water conditions, some cases of high EC soils (e.g., smectite clays) still remain problematic for such TDR sensors (Schwartz et al., 2013; 2016; and Vaz et al, 2013). For example, the adoption of AP by the USCRN in 2019 has not entirely resolved the relatively poor sensor performance occurring at some of the network sites with consistently wet high clay content soils (Wilson et al., 2020). In that study and in this one, the use of factory-supplied calibration developed for loam soils was appropriate to determine VWC by all three sensors within the testbed. The hourly variations of VWC measured by the sensors followed the observed gravimetric soil water that varied with the effects of precipitation, evapotranspiration and drainage. While the use of the factory-supplied calibration equations for loamy soil was successful in determining VWC by both HP and AP within the testbed, it resulted in relatively low VWC measurements by SP. The RMSD in VWC measurements by SP at 10 cm and gravimetric soil water was about 10 $\%m^3$ m^{-3}, compared with RMSD of about 2 $\%m^3$ m^{-3} for HP and AP, and the SP VWC measurements were typically about 9 $\%m^3$ m^{-3} lower than the gravimetric measurements. Because HP and AP were only deployed at 10 cm, we could not compare all three sensors at depths of 20, 30, 40 and 50 cm. However, in the examination of VWC measurements by SP at depths of 30, 40 and 50 cm, the difference between measured values and gravimetric soil water content was less than 4 $\%m^3$ m^{-3}. Future study is therefore needed to evaluate all three sensors at the various depths of SP.

Even though in this study measurements by HP and AP were not available at all the depths of the SP measurements, VWC measurements by all three sensors at 10 cm within the testbed were consistent with results from the small number of reported evaluations of SP found in the literature. Marek et al. (2021) reported lower VWC measurements by 100-cm long SP, when AP measurements were compared with those of SP at all depths in an irrigation scheduling study. Sanchez-Mejia et al. (2020) used a Cosmic-Ray Neutron Sensor (CRNS) to evaluate a 50-cm long SP for VWC measurements in a flood irrigated wheat field with high clay content (~50%) soils in the semiarid Yaqui Valley in northwest Mexico. They found that the SP VWC measurements were also low, with the regression relationship in VWC measurements between CRNS and SP indicating slope = 0.83, R^2 = 0.73, and intercept = 6 $\%m^3$ m^{-3}. Unlike SP, HP and AP are widely used in many soil moisture monitoring networks, and their performance has been evaluated in many studies. Cosh et al. (2016) reported reductions in RMSD from 4 to 2.9 $\%m^3$ m^{-3} for HP and from 8 to 2.5 $\%m^3$ m^{-3} for AP when transitioning from the factory-supplied calibrations to soil-specific calibrations. They included the HP and AP-TDT (time domain transmission) among 11 sensor types used to measure soil moisture profiles within 100-cm of the soil surface at a SMAP satellite testbed near Marena, Oklahoma with well-drained silty clay loam soils. Vaz et al. (2013) evaluated eight commercially available probes in the laboratory in soil containers (12-cm inside diameter and 20.3 cm tall), each with one of six mineral soil types and one organic soil with varying surface specific area (SSA) and EC. They found that the TDR100 probe performed well in the organic soil (RMSD of 1.3 $\%m^3$ m^{-3}) and in all the mineral soils (with average RMSD of 2.3 $\%m^3$ m^{-3}); the HP with the factory-supplied loam calibration equation worked well in the sandy soil (93% Sand) (RMSD = 1.8 $\%m^3$ m^{-3}), but then overpredicted the observed soil water content in the other mineral soils, especially for the soil with 28% clay, 63% silt, SSA of 22 m^2 g^{-1}, and a high EC of 8.39 dS m^{-1}. Ojo et al. (2015) found a large improvement in the HP measurements when comparing the factory-supplied calibration to soil-specific calibrations; the RMSD decreased from 12.9 $\%m^3$ m^{-3} to 1.4 $\%m^3$ m^{-3} for a field with high clay soils (71% clay) in Winnipeg, Canada.

In spite of the low EC measurements in our testbed study, which did not noticeably affect the use of the factory-supplied loam equation, EC values displayed variability with VWC that was consistent with results of similar sensor evaluations. For example, Saarenketo (1998) used soil samples with four different clay mineral types, and varying densities, particle sizes, specific surface areas, and CEC to make dielectric permittivity and electrical conductivity measurements at frequencies ranging from 50 MHz to 3 GHz. The Saarenketo (1998) water content also ranged from dry to wet. He found that the dielectric permittivity for dry soils for all the clays was low, with constant values at frequencies that ranged from 30 MHz to 3.0 GHz. But with soils dominated by 20% clay content of the clay mineral Kaolinite chlorite (mean particle size of 13 μm) with the low CEC of 3.2 meq/100g and specific surface area value of 23,977 m^2/kg, the electrical conductivity displayed only slight increase with water content and did not

affect measurements of dielectric properties over the range of sensor frequency and water content. On the other hand, when soils were dominated by a 38% sticky, plastic, high swelling clay content of the clay mineral quartz muscovite (mean particle size of 3.5 µm) with relatively high CEC of 38.2 meq/100g and large specific surface area of 43,785 m^2/kg, the electrical conductivity exhibited a strong increase with water content. In this example, the measured dielectric permittivity was high, with dielectric permittivity values reaching over 100 in saturated soils at frequency of 50 MHz. Such permittivity values are much higher than the permittivity value of pure water (81). Dielectric permittivity values greater than 81 have also been measured in wet soils with clays that displayed high electrical conductivity (Wilson et al., 2020; Campbell, 1990). When Seyfried et al. (2005) evaluated the HydraProbe in 19 different soil samples that comprised 3 to 63% clay content with different mineralogies, they found no significant correlation between clay content and change in water content. This result was consistent with findings by Campbell (1990) and Saarenketo (1998), who reported that dielectric permittivity measurements in soils with clays are more affected by clay properties such as the CEC and the specific surface area related to the clay mineralogies than by the clay content in the soil. However, we evaluated in this study three sensors that include measurements of EC with measurements of permittivity and temperature. Improved evaluations of these sensors may be fostered by finding ways to assess soil electrical conductivity measurements to address the confounding effects associated with site-specific soil factors (Schwartz et al., 2013; 2016).

Despite the encouraging performance of the three electromagnetic sensors in the measurements of VWC in this study, testbed sensor evaluations have some limitations in their applicability to network operations, particularly long-term regional and national networks. This is due to the distribution of stations across complex and varied soil situations. As a result, factory-supplied calibration equations are often used by networks, including the USCRN, the USDA's Soil Climate Analysis Network (SCAN) (Schaefer, Cosh, & Jackson, 2007), and state mesonets (Mahmood & Foster, 2008; Shulski et al., 2018). The difficulty of obtaining gravimetric soil water measurements throughout a large operational network hinders the implementation of site-specific calibrations. Moreover, explicitly integrating the effect of electrical conduction into the calibration equation in converting measurements of permittivity to VWC remains challenging. However, a better understanding of the role of site-specific soil factors in permittivity measurements is needed to enhance the adoption of select sensors for providing site-specific VWC.

4. Conclusions

Three commercial-grade electromagnetic sensors were used in an open field testbed dedicated to the evaluation of *in situ* measurements of soil water content and soil temperature. Evaluations of sensor results from the period of March 2021 to March 2022 showed that HP and AP performed better than the SP in the measurements of VWC, while all three sensors were nearly equal in the

measurement of the soil temperature. This study clearly supports the finding by Wilson et al. (2020), which validated the performance of AP against the HP at the same testbed site. Measurements of the electrical conductivity by the three sensors showed similarly low values; values that were less than 0.3 S m^{-1}, which varied with VWC. The HP and AP showed relatively equal performance in VWC measurements, with good agreement with the observed gravimetric soil water in the top 10 cm. The SP VWC measurements were generally lower than the HP, AP, and gravimetric measurements. The VWC data demonstrated that the dynamics of evapotranspiration and drainage were much greater in the top 5, 10 and 20 cm depths than in the bottom 30, 40 and 50 cm depths. Therefore, the variability of VWC was much larger in the top 5, 10 and 20 cm than in the 30, 40 and 50 cm depths. The design of the sensing rods of the HP and AP may have allowed for both sensors to better represent the variability in the top 10 cm, which may have led to good agreement between their VWC measurements and the gravimetric soil water. On the other hand, VWC measurements in the top 10 cm by SP were systematically lower than the gravimetric soil water content. This discrepancy suggests a potential shortcoming for the SP sensing rods, as the SP sampling volumes may not have correctly represented the amount of gravimetric water content in the top 10 cm.

Further evaluation of the HP, AP and SP using the testbed study from 2021 to 2022 showed that all three sensors performed similarly in the measurement of EC. Measurements of EC were low, with values less than 0.3 S m^{-1}, which increased slightly with depth. Variability of EC was associated with changes in VWC. The variability of EC with VWC might be important in cases with high EC values, because high EC values in wet soil conditions are known to hinder the operation of electromagnetic sensors (Schwartz et al., 2013; 2016). Laboratory and field studies have demonstrated how EC can influence dielectric permittivity measurements to determine VWC, and many of these studies have revealed that high EC in some clay soils may affect sensors like the HP more than with TDR sensors like the AP and SP (Burns et al., 2014; Vaz et al., 2013; Logsdon et al., 2010; Kelleners et al., 2009).

The testbed in this study was designed to focus on a coarse loam soil. Additional study is needed to extend the evaluation of SP alongside HP and AP to other soil environments, including high clay soils with high electrical conductivity. In addition, HP and AP were located only at a depth of 10 cm, and it was not possible to evaluate them against the SP at depths of 5, 20, 30, 40 and 50 cm. Notwithstanding, the results of this study indicate that SP may be useful for monitoring the soil temperature profile, particularly when accurate VWC measurement is less essential.

Acknowledgments

References

Bell, J.E., M.A. Palecki, C.B. Baker, W.G. Collins, J.H. Lawrimore, R.D. Leeper, et al. 2013. U.S. Climate Reference Network soil moisture and temperature observations. J. Hydrometeorol. 14:977–988. doi:10.1175/JHM-D-12-0146.1

Blonquist, J. M., S. B. Jones, and D. A. Robinson. 2005. Standardizing Characterization of Electromagnetic Water Content Sensors. Vadose Zone J. 4:1059-1069. doi:10.2136/vzj2004.0141

Bohn, H.L., B.L. McNeal, G.A. O'Conner. 1985. Soil Chemistry. 2nd ed. John Wiley & Sons, New York.

Brye, K.R., J.M. Norman, and L.G. Bundy. 2000. Water-budget evaluation of prairie and maize ecosystems. Soil Sci. Soc. Am. J. 64:715-724.

Burns, T. T., J. R. Adams, and A. A. Berg. 2014. Laboratory Calibration Procedures of the Hydra Probe Soil Moisture Sensor: Infiltration Wet-Up vs. Dry-Down. *Vadose Zone J.* 13. doi:10.2136/vzj2014.07.0081.

Caldwell, T. G., T. Bongiovanni, M. H. Cosh, C. Halley, and M. H. Young. 2018. Field and Laboratory Evaluation of the CS655 Soil Water Content Sensor. Vadose Zone J. 17:170214. doi:10.2136/vzj2017.12.0214.

Caldwell, T. G., T. Bongiovanni, M.H. Cosh, T.J. Jackson, A. Colliander, C.J. Abolt, R. Casteel, T. Larson, B.R. Scanlon, and M.H. Young, M. H. 2019. The Texas soil observation network: A comprehensive soil moisture dataset for remote sensing and land surface model validation. Vadose Zone J., 18: 1-20 190034. https://doi.org/10.2136/vzj2019.04.0034

Campbell, J.J. 1990. Dielectric properties and influence of conductivity in soils at on to fifty megahertz. Am. J. Soil Sci. 54:332-341.

Cheng, W. Y. Y. and W.R. Cotton. 2004. Sensitivity of a Cloud-Resolving Simulation of the Genesis of a Mesoscale Convective System to Horizontal Heterogeneities in Soil Moisture Initialization. J. Hydrometeorol., 5(5): 934-958.

Chen, Y. and D. Or. 2006. Geometrical factors and interfacial processes affecting complex dielectric permittivity of partially saturated porous media. Water resources res., 42(6):1-9.

Crow, W.T. and E.F Wood. 2002. The value of coarse-scale soil moisture observations for regional Surface energy balance modeling. J. Hydrometeorol. 3(4): 467–82. http://www.jstor.org/stable/24909194.

Cosh, M. H., T. E. Ochsner, L. McKee, J. Dong, J. B. Basara, S. R. Evett, C. E. Hatch, E. E. Small, S. C. Steele-Dunne, M. Zreda, and C. Sayde. 2016. The Soil Moisture Active Passive Marena, Oklahoma, In Situ Sensor Testbed (SMAP-MOISST): Testbed Design and Evaluation of In Situ Sensors. Vadose Zone J. 15. doi:10.2136/vzj2015.09.0122

Diamond, H.J., T.R. Karl, M.A. Palecki, C.B. Baker, J.E. Bell, R.D. Leeper, et al. 2013. U.S. Climate Reference Network after one decade of operations. Bull.

Am. Meteorol. Soc. 94:485–498. doi:10.1175/BAMS-D-12-00170.1

Dettmann, U., and M. Bechtold. 2018. Evaluating Commercial Moisture Probes in Reference Solutions Covering Mineral to Peat Soil Conditions. Vadose Zone J. 17:170208. doi:10.2136/vzj2017.12.0208

Evett, S. R., J. A. Tolk, and T. A. Howell. 2005. Time Domain Reflectometry Laboratory Calibration in Travel Time, Bulk Electrical Conductivity, and Effective Frequency. Vadose Zone J. 4:1020-1029. doi:10.2136/vzj2005.0046

Evett, S.R., J.A. Tolk, and T.A. Howell. 2006. Soil profile water content determination: Sensor accuracy, axial response, calibration, temperature dependence, and precision. Vadose Zone J. 5:894–907.

Hubbard, K.G. and H. Wu. 2005. Modification of a crop-specific drought index for simulation corn yield in wet years. Agron. J. 97:1478-1484.

James, S. E., M. Pärtel, S.D. Wilson, and D.A. Peltzer. 2003. Temporal heterogeneity of soil moisture in grassland and gorest. J. Ecol. 91, no. 2 (2003): 234–39. http://www.jstor.org/stable/3599758.

Jones, A.S., Aanderud, Z.T., Horsburgh, J.S., Eiriksson, D.P., Dastrup, D., Cox, C., Jones, S.B., Bowling, D.R., Carlisle, J., Carling, G.T. and Baker, M.A., 2017. Designing and implementing a network for sensing water quality and hydrology across mountain to urban transitions. J. Amer. Water Resourc. Assoc. 53(5):1095-1120.

Jones, S. B., J. M. Blonquist, D. A. Robinson, V. P. Rasmussen, and D. Or. 2005. Standardizing Characterization of Electromagnetic Water Content Sensors. Vadose Zone J. 4:1048-1058. doi:10.2136/vzj2004.0140

Logsdon, S.D. and D.A. Laird. 2004. Electrical conductivity spectra of smectites as influenced by saturating cation and humidity. Clays and clay minerals, 52(4):411-420.

Logsdon, S. D., T.R. Green, M. Seyfried, S.R. Evett, and J. Bonta. 2010. Hydra probe and twelve-wire probe comparisons in fluids and soil cores. Soil Science Society of America Journal, 74, 5–12. https://doi.org/10.2136/sssaj2009.0189

Mahmood, R. and S.A. Foster. 2008. Mesoscale weather and climate observations in Kentucky for societal benefit. Focus on Geography, 50, 32–36. https://doi.org/10.1111/j.1949-8535.2008. tb00210.x

Marek, G.W., Evett, S.R., Marek, T.H., Heflin, K.R., Bell, J., Brauer, D.K. 2021. Field evaluation of conventional and downhole TDR soil water sensors for irrigation scheduling in a clay loam soil [abstract]. ASABE Annual International Meeting, Virtual and On-Demand, July 12-16, 2021. Virtual Presentation No. 2101085.

Mittelbach, H., F. Casini, I. Lehner, A.J. Teuling, and S.I. Seneviratne. 2011. Soil moisture monitoring for climate research: Evaluation of a low-cost sensor in

the framework of the Swiss Soil Moisture Experiment (SwissSMEX) campaign. J. Geophys. Res., 116(D5).

Moeletsi, M.E. and S. Walker. 2012. Assessment of agricultural drought using a simple water balance model in the Free State Province of South Africa. Theor Appl. Climatol 108:425–450. https://doi.org/10.1007/s00704-011-0540-7

Morgan, C.L.S., J.M. Norman, and B. Lowery. 2003. Estimating plant-available water across a field with an inverse yield model. Soil Sci. Soc. Am. J. 67:620-629

NIDIS. 2019. Nation Integrated Drought Information System (NIDS) Program Bill (online). Available at https://www.congress.gov/bill/115th-congress/senate-bill/2200 (President signed S.2200 into law, Jan. 7, 2019).

Or, D. and J.M. Wraith. 1999. Temperature effects on soil bulk dielectric permittivity measured by time domain reflectometry: A physical model. Water Resources Res., 35(2):371-383.

Roberti, J. A., E. Ayres, H.W. Loescher, J. Tang, G. Starr, D.J. Durden, … C.R. Zulueta. 2018. A robust calibration method for continental-scale soil water content measurements. Vadose Zone Journal, 17, 1–19. https://doi.org/10.2136/vzj2017.10.0177

Robinson, D.A., C.S. Campbell, J.W. Hopmans, B.K. Hornbuckle, S.B. Jones, R. Knight, F. Ogden, J. Selker, and O. Wendroth. 2008. Soil moisture measurement for ecological and hydrological watershed-scale observatories: A review. Vadose Zone J. 7:358-389.

Robinson, D.A., Jones, S.B., Wraith, J.M., D. Or, and S.P. Friedman. 2003. A review of advances in dielectric and electrical conductivity measurement in soils using time domain reflectometry. Vadose Zone J., 2(4):444-475.

Saarenketo, T. 1998. Electrical properties of water in clay and silty soils. J. Appl. Geophys. 40:73-88.

Sanchez-Mejia, Z., E. Yepez, F. Gaxiola, O.P. Rubio, J.R.T. Velázquez, J.C. Alvarez-Yepiz, and J. Garatuza-Payan. 2020. Flood irrigation agriculture: The challenges of in-situ soil moisture monitoring in lands with high clay contentA. Washington: American Geophysical Union. doi:https://doi.org/10.1002/essoar.10505315.1

Schaefer, G. L., H.M. Cosh, and T.J. Jackson. 2007. The USDA Natural Resources Conservation Service Soil Climate Analysis Network (SCAN). Journal of Atmospheric and Oceanic Technology, 24, 2073–2077. https://doi.org/10.1175/2007JTECHA930.1

Schwartz, R. C., S.R. Evett, M.G. Pelletier, and J.M. Bell. 2009. Complex Permittivity Model for Time Domain Reflectometry Soil Water Content Sensing: I. Theory. Soil Sci. Soc. Am. J., 73: 886-897. https://doi.org/10.2136/sssaj2008.0194

Schwartz, R. C., S. R. Evett, S. K. Anderson, and D. J. Anderson. 2016. Evaluation of a Direct-Coupled Time-Domain Reflectometry for Determination of Soil Water Content and Bulk Electrical Conductivity. Vadose Zone J. 15. doi:10.2136/vzj2015.08.0115

Schwartz, R. C., J.J. Casanova, M.G. Pelletier, S.R. Evett, and R.L. Baumhardt. 2013. Soil Permittivity Response to Bulk Electrical Conductivity for Selected Soil Water Sensors. Vadose Zone J. 12. doi:10.2136/vzj2012.0133

Sciuto, G. and B. Diekkruger. 2010. Influence of soil heterogeneity and spatial discretization on catchment water balance modeling. Vadose Zone J. 9:955-969.

Shulski, M. S. Cooper, G. Roebke, and A. Dutcher. 2018. The Nebraska Mesonet: Technical overview of an automated state weather network. Journal of Atmospheric and Oceanic Technology, 35, 2189–2200. https://doi.org/10.1175/JTECH-D-17-0181.1

Seyfried, M. S., and L.E. Grant. 2007. Temperature effects on soil dielectric properties measured at 50 MHz. Vadose Zone J. 6:759-765.

Seyfried, M. S., and M. D. Murdock. 2004. Measurement of Soil Water Content with a 50-MHz Soil Dielectric Sensor. Soil Sci. Soc. Am. J. 68:394-403. doi:10.2136/sssaj2004.3940

Seyfried, M.S., L.E. Grant, E. Du, and K. Humes. 2005. Dielectric loss and calibration of the Hydra Probe soil water sensor. Vadose Zone J. 4:1070–1079. doi:10.2136/vzj2004.0148

Shulski, M., S. Cooper, G. Roebke, and A. Dutcher, 2018: The Nebraska Mesonet: Technical Overview of an Automated State Weather Network. J. Amos. Oceanic Technol., 35:2189-2200. doi:10.1175/JTECH-D-17-0181.1

Stevens Water Monitoring Systems, Inc. 2018. Comprehensive Stevens Hydra Probe II User's Manual. www.stevenswater.com, Stevens Water Monitoring Systems, Inc., Portland, OR, USA.

Topp, G.C., S. Zegelin, and I. White. 2000. Impacts of the Real and Imaginary Components of Relative Permittivity on Time Domain Reflectometry Measurements in Soils. Soil Sci. Soc. Am. J. 64:1244-1252. doi:10.2136/sssaj2000.6441244x

Torres, G.M., R.P. Lollato, and T.E. Ochsner. 2013. Comparison of drought probability assessments based on atmospheric water deficit and soil water deficit. Agron. J. 105:428-436.

Vaz, C. M.P., S. Jones, M. Meding, and M. Tuller. 2013. Evaluation of Standard Calibration Functions for Eight Electromagnetic Soil Moisture Sensors. Vadose Zone J. 12. doi:10.2136/vzj2012.0160

Wilson, T. B., C. B. Baker, T. P. Meyers, J. Kochendorfer, M. Hall, J. E. Bell, H. J. Diamond, and M. A. Palecki. 2016. Site-Specific Soil Proper-

ties of the US Climate Reference Network Soil Moisture. Vadose Zone J. 15. doi:10.2136/vzj2016.05.0047

Wilsona, T.B., H.J. Diamond, J. Kochendorfer, et al. 2020. Evaluating time domain reflectometry and coaxial impedance sensors for soil observations by the U.S. Climate Reference Network. *Vadose Zone J.* 2020; 19:e20013. https://doi.org/10.1002/vzj2.20013

List of Figures

List of Tables

2. The mean absolute percentage difference (MAPD) and the root mean square difference (RMSD) relative to mean of soil temperature measured by the individual HydraProbes (HP), Acclima TDR Probes (AP), and SoilVUE10 TDR Probe (SP) at six depths of 5 to 50 cm inside the testbed during 2021 to 2022.

3. The mean absolute percentage difference (MAPD) and the root mean square difference (RMSD) relative to mean of volumetric water content (VWC) measured by the individual HydraProbes (HP), Acclima TDR Probes (AP), and SoilVUE10 inside the testbed at six depths of 5 to 50 cm during 2021 to 2022.
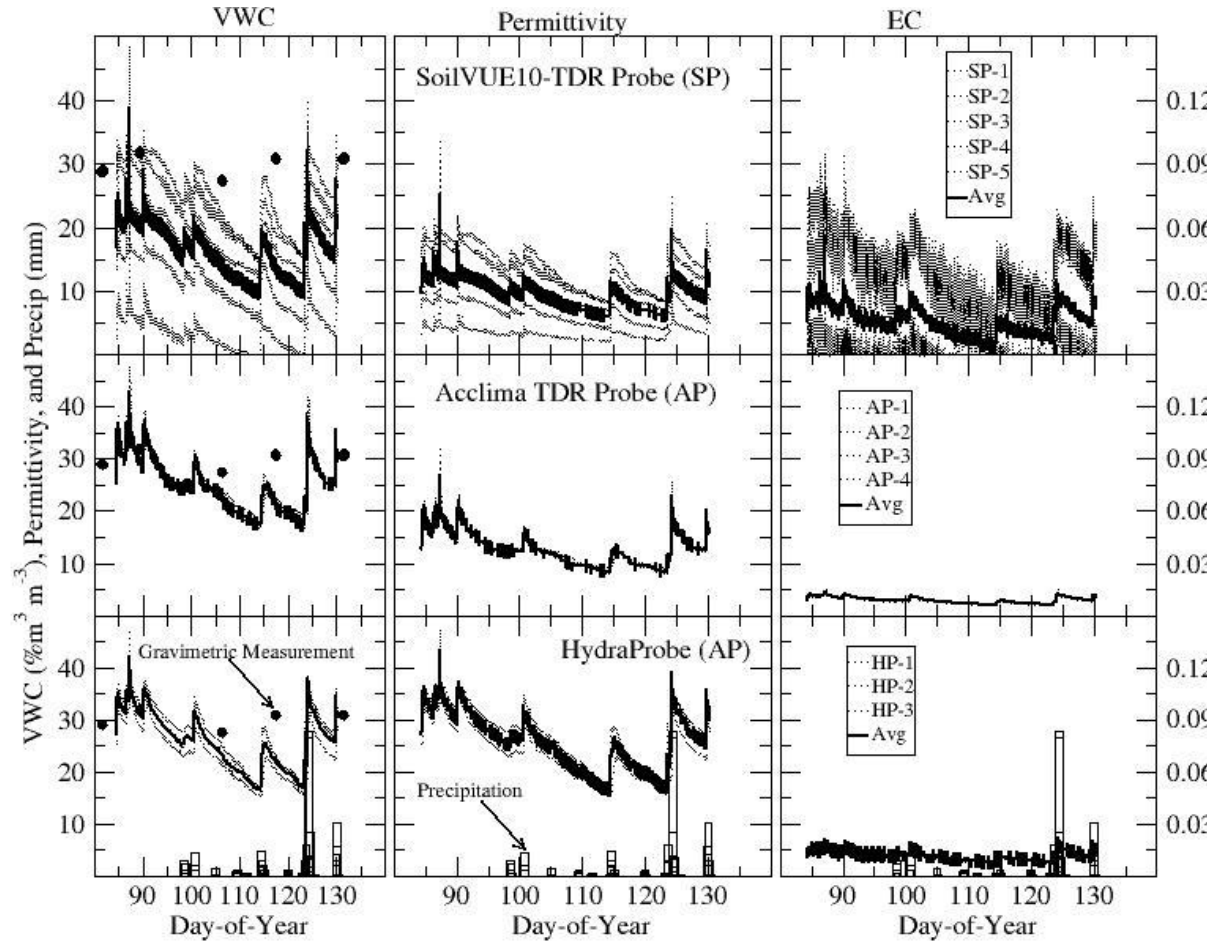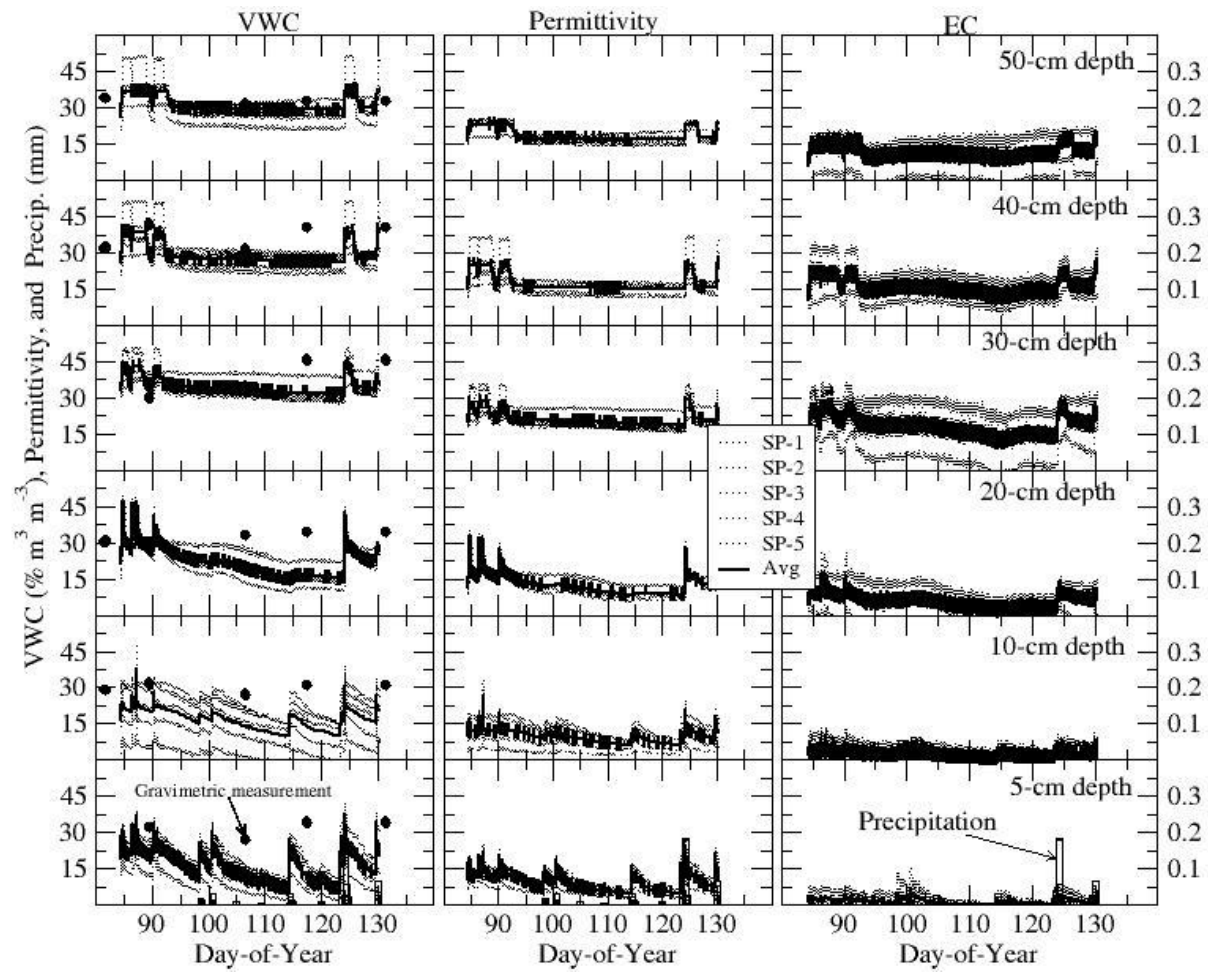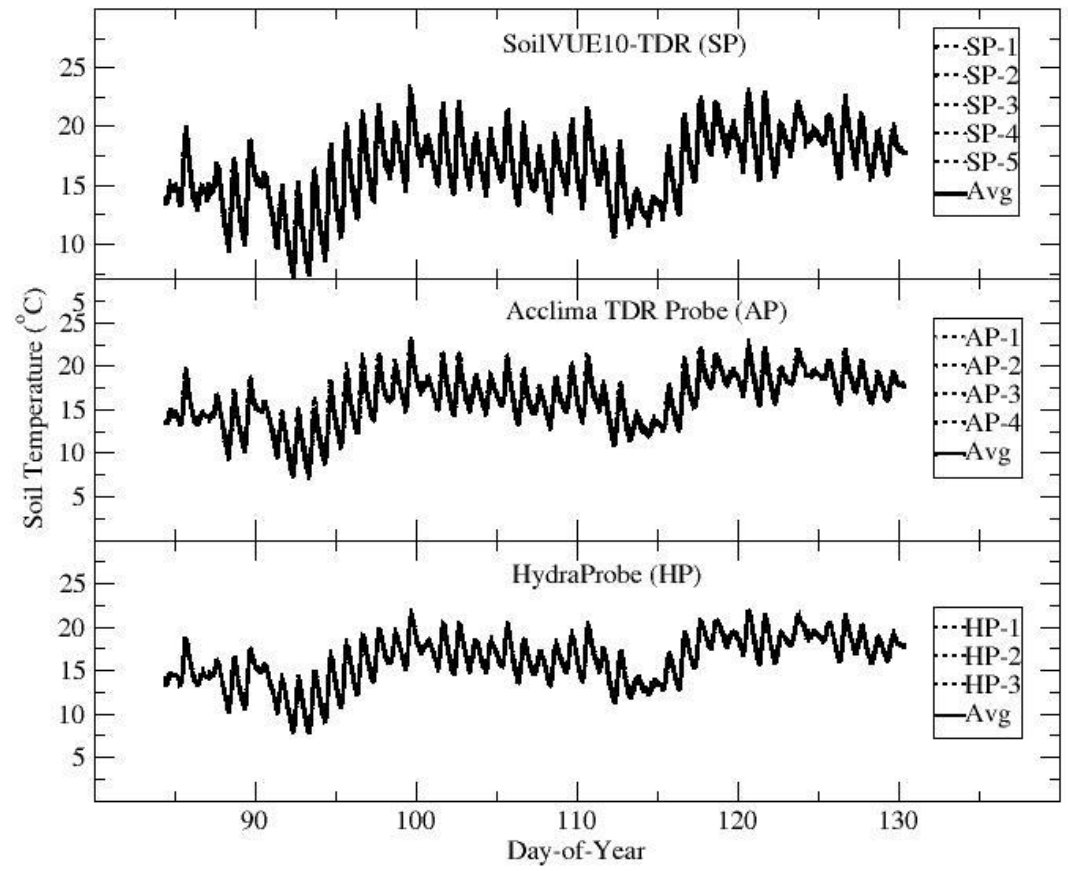

Fig. 1

21

Fig. 2

Fig. 3

Fig. 4

The scatter plot shows Soil Temperature HP/SP (°C) on the y-axis versus Soil Temperature for AP (°C) on the x-axis, both ranging from 0 to 30.

		Slope	R^2	Interpt	RMSD
HP	∘	0.99	0.99	0.05	0.13
SP	⋄	1.01	0.99	0.14	0.32

Fig. 5

25

VWC (%m³ m⁻³)   Soil Temperature (°C)   EC (S m⁻¹)

Mean Gravimetric

Mean measured by SP
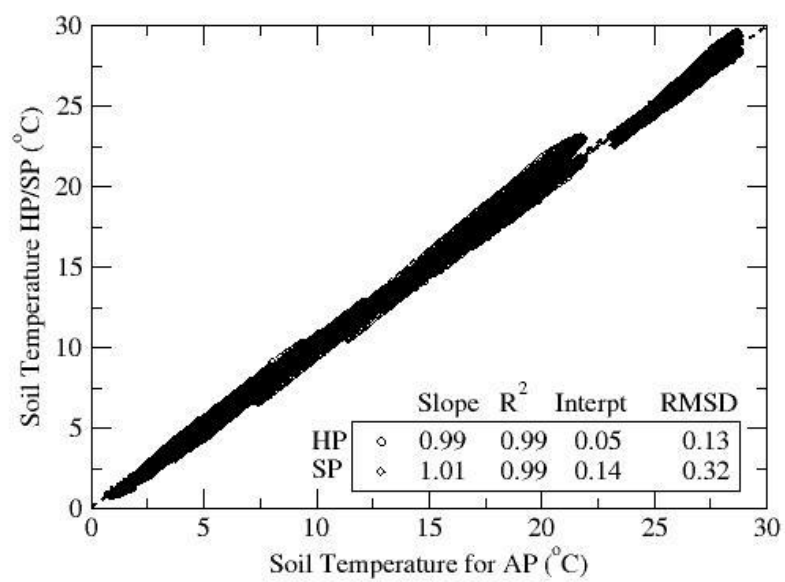
Mean measured by SP

Mean measured by SP

Depth (cm)

Fig. 6

26
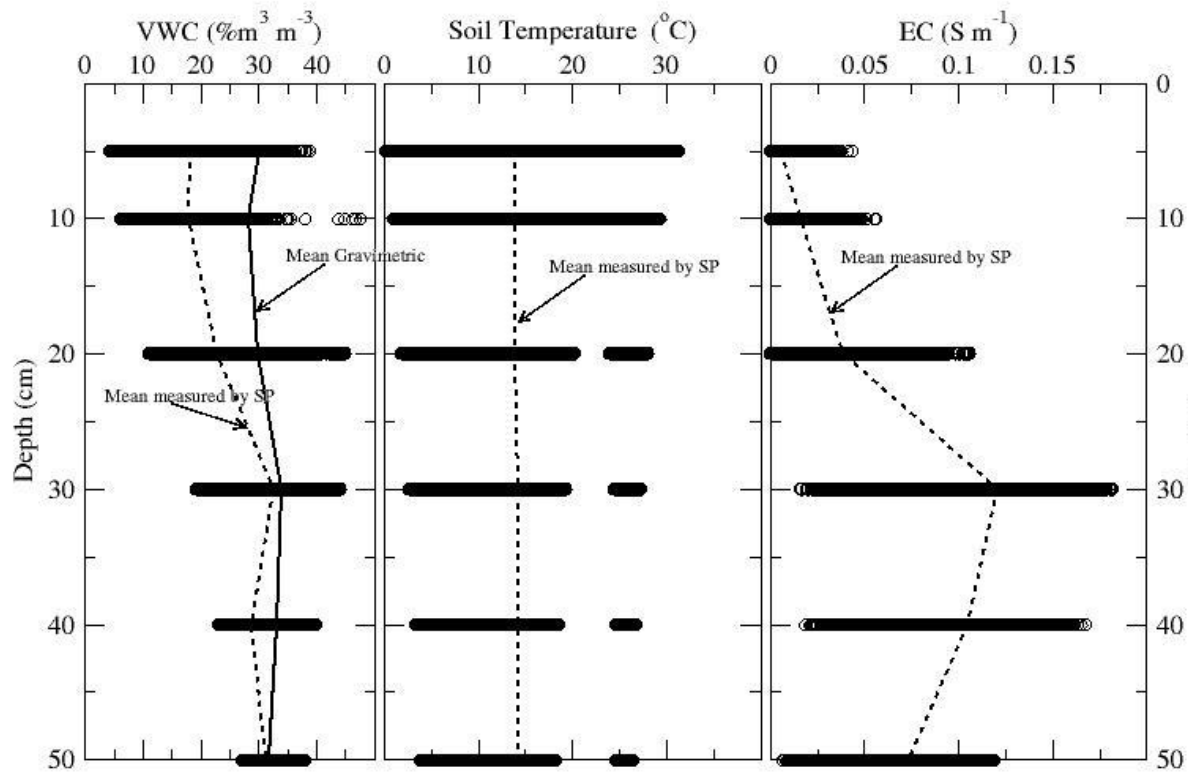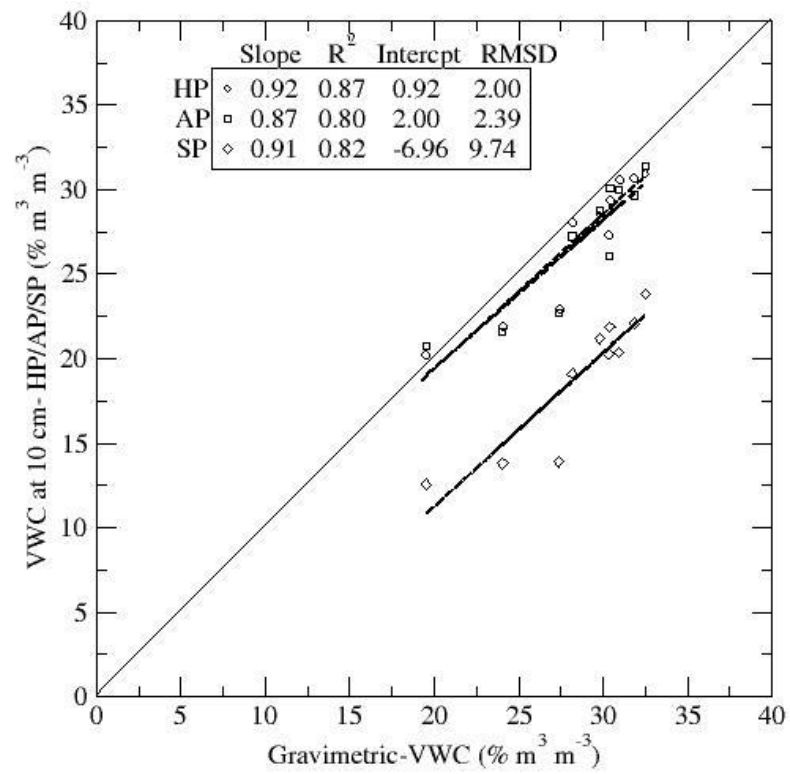
Fig. 7

Fig. 8

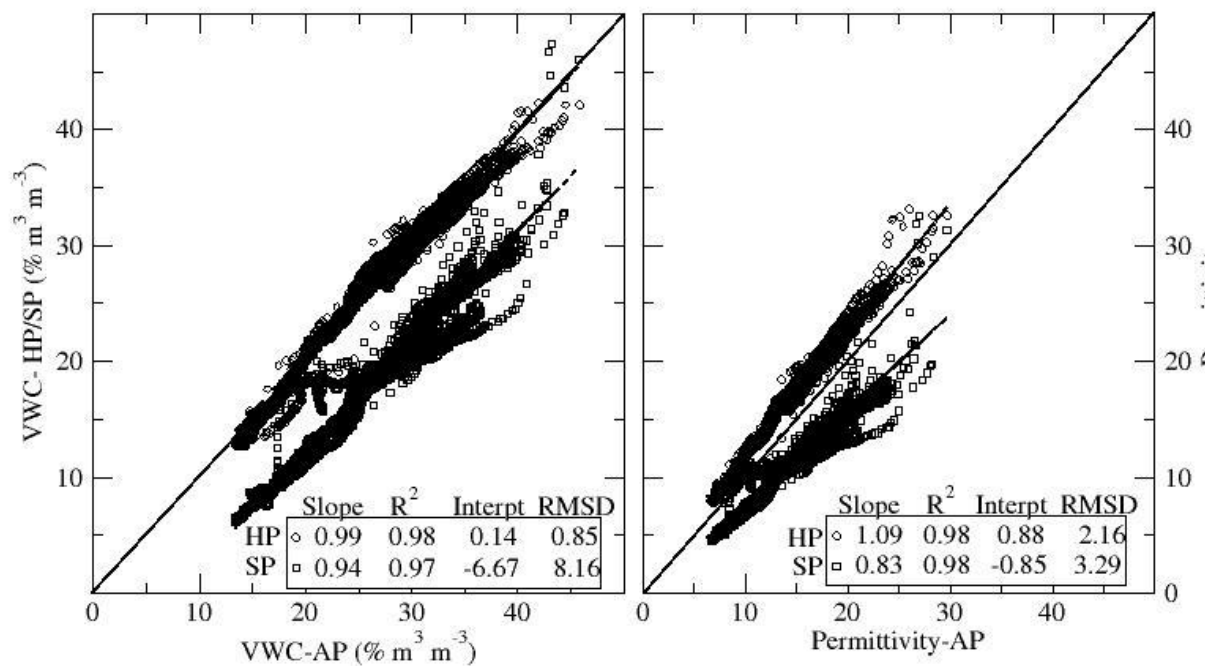Table 1. Gravimetric volumetric water content measurements obtained alongside measurements by SP at six depths from 5 to 50 cm inside the testbed during 2021 to 2022.

@ >p(- 16) * >p(- 16) * >p(- 16) * >p(- 16) * >p(- 16) * >p(- 16) * >p(-16) * >p(- 16) * >p(- 16) * @ & & -------- Volumetric water Content ------- & & & & & & &

Depth (cm) =

&

-05-

& -10- & -20- & -30- & -40- & -50- & &

28

BD (g cm⁻³) =							

BD (g cm^{-3}) =
& (1.09) & (1.21) & (1.32) & (1.35) & (1.40) & (1.58) & &

Date
&
Hour
& ------------------- (% m^3 m^{-3}) -------------------- & Methods & & & & &

03/30/2021
&
1200
& 20.60 & 20.16 & 27.92 & 35.32 & 29.48 & 37.00 & SP
& & 32.01 & 31.85 & 30.55 & 30.16 & 42.05 & 37.46 & Gravimetric

04/16/2021
&
1200
& 12.02 & 13.90 & 19.32 & 33.56 & 27.28 & 29.32 & SP
& & 26.79 & 27.40 & 33.06 & 33.26 & 31.65 & 31.74 & Gravimetric

04/27/2021
&
1200
& 12.34 & 13.80 & 16.32 & 31.84 & 26.44 & 29.46 & SP
& & 26.26 & 24.05 & 23.80 & 40.58 & 30.93 & 31.18 & Gravimetric

05/11/2021
&
1200

& 22.52 & 20.40 & 26.78 & 36.32 & 38.7 & 37.50 & SP
& & 34.39 & 30.93 & 34.31 & 45.89 & 40.47 & 32.90 & Gravimetric

05/25/2021

&

1100

& 13.79 & 14.82 & 16.03 & 25.49 & 25.38 & 25.32 & Gravimetric
&

1100

& 30.02 & 31.63 & 33.87 & --- & --- & --- & Gravimetric

06/22/2021

&

1200

& 19.60 & 19.10 & 21.50 & 29.92 & 25.92 & 29.12 & SP

07/20/2021

&

1200

& 31.29 & 28.17 & 35.44 & --- & --- & --- & Gravimetric
&

1300

& 23.34 & 21.88 & 27.70 & 36.24 & 31.86 & 35.66 & SP

12/20/2021

& & 33.87 & 30.41 & 27.78 & 31.32 & --- & --- & Gravimetric

01/04/2022

&

1600

& 24.84 & 23.84 & 30.90 & 38.96 & 39.32 & 36.88 & SP
& & 40.11 & 32.51 & 33.42 & 36.27 & --- & --- & Gravimetric

02/21/2022

&

1300

& 22.60 & 29.00 & 25.20 & 33.40 & 29.50 & 29.70 & SP
& & 32.04 & 29.80 & 30.55 & 29.17 & 28.92 & --- & Gravimetric

Table 2. The mean absolute percentage difference (MAPD) and the root mean square difference (RMSD) relative to mean of soil temperature measured by the individual HP, AP, and SP at six depths of 5 to 50 cm within the testbed during 2021 to 2022.

@ >p(- 24) * >p(- 24) * >p(- 24) * >p(- 24) * >p(- 24) * >p(- 24) * >p(- 24) * >p(- 24) * >p(- 24) * >p(- 24) * >p(- 24) * >p(- 24) * >p(- 24) * @

Depth

& ------------------- MAPD ------------------- & & ---------------- RMSD ---------------- & & & & & & & & &
&

Sens1

& Sens2 & Sens3 & Sens4 & Sens5 & & Sens1 & Sens2 & Sens3 & Sens4 & Sens5 & Type

(cm)

&

(%)

& (%) & (%) & (%) & (%) & & (C) & (C) & (C) & (C) & (C) &

05

& 1.54 & 1.83 & 1.10 & 1.76 & 1.99 & & 0.30 & 0.40 & 0.22 & 0.26 & 0.31 & SP

10

& 1.13 & 1.16 & 0.90 & 1.29 & 1.82 & & 0.21 & 0.21 & 0.19 & 0.17 & 0.27 & SP

10

& 3.90 & 5.16 & 1.98 & -- & -- & & 0.27 & 0.30 & 0.17 & -- & -- & HP

10

& 1.74 & 4.00 & 2.60 & 3.89 & -- & & 0.32 & 0.36 & 0.61 & 0.37 & -- & AP

20

& 0.84 & 0.88 & 0.81 & 0.85 & 1.62 & & 0.12 & 0.14 & 0.13 & 0.13 & 0.26 & SP

30

& 0.60 & 0.81 & 0.79 & 0.83 & 1.31 & & 0.09 & 0.14 & 0.12 & 0.12 & 0.22 & SP

40

& 0.33 & 0.78 & 0.66 & 0.73 & 0.95 & & 0.05 & 0.14 & 0.11 & 0.11 & 0.16 & SP

50

& 0.37 & 0.44 & 0.62 & 0.58 & 0.74 & & 0.07 & 0.07 & 0.10 & 0.09 & 0.13 & SP

Table 3. The mean absolute percentage difference (MAPD) and the root mean square difference (RMSD) relative to the mean of volumetric water content (VWC) measured by the individual HP, AP, and SP within the testbed at six depths of 5 to 50 cm during 2021 to 2022.

@ >p(- 24) * >p(- 24) * >p(- 24) * >p(- 24) * >p(- 24) * >p(- 24) * >p(- 24) * >p(- 24) * >p(- 24) * >p(- 24) * >p(- 24) * >p(- 24) * >p(- 24) * @

Depth

& ------------------ MAPD ------------------- & & --------------- RMSD ---------------- & & & & & & & & &
&

Sens1

& Sens2 & Sens3 & Sens4 & Sens5 & & Sens1 & Sens2 & Sens3 & Sens4 & Sens5 & Type

(cm)

&

(%)

& (%) & (%) & (%) & (%) & & (%) & (%) & (%) & (%) & (%) &

05
&

4.89
& 37.49 & 10.31 & 38.20 & 9.91 & & 1.11 & 6.75 & 1.73 & 6.21 & 2.10 & SP

10
& 47.72 & 65.17 & 21.73 & 25.37 & 13.81 & & 8.17 & 10.91 & 3.63 & 4.22 & 2.62 & SP

10
& 5.33 & 8.71 & 4.04 & --- & --- & & 1.58 & 2.40 & 1.14 & --- & --- & HP

10
& 2.79 & 1.60 & 1.07 & 1.68 & --- & & 0.97 & 0.60 & 0.49 & 0.55 & --- & AP

20
& 3.24 & 10.70 & 7.30 & 30.72 & 13.62 & & 1.02 & 2.66 & 1.67 & 6.49 & 3.08 & SP

30
& 3.76 & 8.20 & 3.90 & 6.83 & 18.30 & & 1.68 & 2.78 & 1.64 & 2.51 & 5.93 & SP

40
& 7.03 & 12.25 & 6.43 & 14.06 & 13.02 & & 2.36 & 3.66 & 1.96 & 4.54 & 4.14 & SP

50
& 4.17 & 8.30 & 7.18 & 2.54 & 12.64 & & 1.78 & 2.67 & 2.36 & 1.00 & 4.20 & SP